ASSESSMENT OF RADIOLOGICAL ENVIRONMENTAL IMPACT UNDER VARIOUS METEOROLOGICAL CONDITION

by

Feifei WU[a,b], Binchi MENG[a,b], Bing LIAN[a,b*], Yan WANG[a,b] and Jing KANG[a,b]

[a] China Institute for Radiation Protection, Taiyuan, China
[b] Key Laboratory of Radiation Environment and Health of the Ministry of Ecology and Environment, Taiyuan, China

Original scientific paper
https://doi.org/10.2298/TSCI2403225W

The meteorological parameters, e.g., wind direction, wind speed and atmospheric stability, affect greatly the diffusion of pollution and radiological environmental impact assessment. Based on the hourly meteorological data obtained from an automatic monitoring station, the radiological impact indicated by the air concentration, individual dose and maximal individual effective dose were analyzed and compared between 2020 and 2021. The paper concluded that children are the main group to be the most easily infected, and the critical exposure path is internal exposure from inhalation. This paper offers a new window for timely decision-making for radiological safety under different climate conditions.

Key words**:** *radiological environmental impact assessment, atmospheric stability, individual effective dose*

Introduction

The radiological environmental impact assessment (REIA) focuses on the effects of radioactive releases on the surrounding environment and population. After the release of a radioactive plume, the radiological impact is assessed by the dose evaluation. According to the *Assessment of the Impact of Radioactive Discharges to the Environment* (SRS 113) issued by International Atomic Energy Agency (IAEA), the total effective dose incorporates all the possible doses from all the delivery pathways, which includes the internal exposure from the inhalation of airborne material, ingestion of foodstuffs, as well as external exposure from immersion in the plume and ground-shine from ground-deposited materials. It is very important to ensure the safety of the environment and the general mass.

In the REIA, the meteorological environment is one of the important factors which influences the dispersion capability of radioactive pollutants and the level of radiation and effective dose [1]. Meteorological parameters such as wind direction, wind speed and atmospheric stability greatly affect the diffusion of pollution. The mountain-river relation [2, 3] will greatly affect the meteorological environment, and a high building and a small moving water channel will affect its local meteorological environment.

The wind direction indicates the initial trajectory of a plume and the subsequent variations in wind intensity and direction will affect the dispersion [4]. Atmospheric stability is used to quantify the dispersion capabilities of the ambient atmosphere [5]. The 3-D joint fre-

* Corresponding author, e-mails: lianbing00@sina.com, wff_bnu@163.com

quencies with the combination of wind direction, wind speed and atmospheric stability are usually used as the input parameter to calculate the individual effective dose.

In the traditional REIA, the 3-D joint frequencies were usually counted using the meteorological data in recent three years. It revealed the radiation effective dose level under the three-average meteorological parameters. However, it is easy to ignore the fact that the effective dose during the whole year will change due to the change of meteorological parameters. To reveal radiological consequences more accurately, it is essential to conduct a refined assessment to reveal the effective dose change under annual meteorological conditions. It can provide suggestions for decision-making by comparing the dose results under different climate scenarios.

Data and methodology

Data description

The hourly meteorological data were obtained from China Meteorological Data Service Center. The automatic meteorological parameters included the temperature, wind direction, wind speed, total solar radiation and nocturnal net radiation. The hourly meteorological data in Mount Emei station between 2020 and 2021 were selected in this study. To evaluate the radiological impact under meteorological variations, the base year was set as 2020 and the assessment year was set as 2021.

Atmospheric stability

Atmospheric stability classification was required to quantify the dispersion capabilities of the ambient atmosphere. Table 1 shows that atmospheric stability in this study was estimated from six different stability classification schemes based on solar radiation during the daytime, nocturnal net radiation, and wind speed at the height of 10 meters [6]. As shown in tab. 1, the atmospheric stability was designated as A (highly unstable), B (moderately unstable), C (slightly unstable), D (neutral), E (moderately stable) and F (extremely stable). From A to F, the atmospheric stability gradually increased whereas the pollutants dispersion weakened.

Table 1. Atmospheric stability classification

Wind speed U [ms^{-1}]	Stability, daytime, solar radiation, R_D [Langley per hour]				Stability, nighttime, nocturnal net radiation R_N [Langley per hour]		
	$R_D \geq 50$	$50 > R_D \geq 25$	$25 > R_D \geq 12.5$	$12.5 > R_D$	$R_N > -1.8$	$-1.8 \geq R_N > -3.6$	$-3.6 \geq R_N$
$U < 2$	A	A-B	B	D	D	–	–
$2 \leq U < 3$	A-B	B	C	D	D	E	F
$3 \leq U < 4$	B	B-C	C	D	D	D	E
$4 \leq U < 6$	C	C-D	D	D	D	D	D
$6 \leq U$	C	D	D	D	D	D	D

Dose calculation model

The hypothetical radioactive releases were considered in this study. The height of the stack was set as 100 meters and the radionuclide U-234 was analyzed in this study. The assessment region was circular with the stack as the center and a radius of 80 km. The assessment region was divided into 192 sub-regions based on 12 concentric circles and 16 ori-

entations. The radius of 12 concentric circles included 1 km, 2 km, 3 km, 5 km, 10 km, 20 km, 30 km, 40 km, 50 km, 60 km, 70 km, and 80 km. Four age classes were considered in this study, which included baby, infant, child and adult groups. The sub-region inhibited was around 5 km from the center.

The exposure pathways considered in the dose assessment for the discharge to the atmosphere included the internal exposure from inhalation of airborne material and ingestion of foodstuffs, as well as the external exposure from immersion in a cloud containing radionuclides and ground-shine from ground-deposited materials in this study. The dose conversion factors (DCF) for the evaluated radionuclides were taken from the recommendations of the IAEA Safety Series No. 113, Radiation Protection Bureau of Health Canada and Atomic Energy Control Board.

The individual effective dose components are given by:

$$\text{Inhalation dose} = \text{DCF}_{\text{inhalation}} \times \text{Air concentration} \times \text{Breathing rate} \quad (1)$$

$$\text{Ground-shine dose} = \text{DCF}_{\text{Ground-shine}} \times \text{Ground deposition} \quad (2)$$

$$\text{Immersion dose} = \text{DCF}_{\text{immersion}} \times \text{Air concentration} \quad (3)$$

$$\text{Ingestion dose} = \text{DCF}_{\text{Ingestion}} \times \text{Intake weight} \quad (4)$$

$$\text{Individual effective dose} = \text{Inhalation dose} + \text{Ground-shine dose} + \text{+ Immersion dose} + \text{Ingestion dose} \quad (5)$$

Results

Analysis of meteorological parameter variations

Table 2 shows the frequency of wind direction in 2020 and 2021 and the change between 2020 and 2021. As shown in tab. 2, the prevailing wind direction was NW. The frequency of calm wind (C) decreased significantly, from 14.31% in 2020 to 6.02% in 2021. In addition, the frequency in five wind directions decreased from 2020 to 2021. In contrast, the frequency in eleven wind directions increased, ranging from 0.17% in the SW wind direction to 2.19% in the SSE wind direction. Though the frequency in each wind direction changed, the prevailing wind direction was consistent between 2020 and 2021. The dispersion of atmospheric pollutants was essentially related to the calm wind conditions. Under decreasingly calm wind conditions, atmospheric pollutant dispersion in 2021 was easier than the last year.

Table 2. Frequency and change of wind direction in 2020 and 2021 [%]

Year	N	NNE	NE	ENE	E	ESE	SE	SSE	S
2020	2.02	7.59	7.96	4.79	4.36	5.27	6.09	5.64	5.68
2021	2.61	8.95	9.71	6.04	6.34	7.09	8.05	7.83	5.97
Change	0.59	1.36	1.75	1.25	1.98	1.82	1.96	2.19	0.29
Year	SSW	SW	WSW	W	WNW	NW	NNW	C	
2020	3.54	2.46	3.53	4.36	5.28	10.89	6.23	14.31	
2021	3.72	2.63	2.9	3.2	3.13	10.01	5.8	6.02	
Change	0.18	0.17	–0.63	–1.16	–2.15	–0.88	–0.43	–8.29	

Atmospheric stability plays a significant role in the dispersion capability of radioactive pollutants. Based on the data from the hourly automated monitoring station, atmospheric stability was analyzed and classified into six classes from highly unstable state (A) to extremely stable state (F). From A to F, the atmospheric stability gradually increased whereas the pollutants dispersion weakened, and this trend was expected to increase the concentration of pollutants and radiological dose impact.

Table 3 shows the proportion of different atmospheric stability classifications in 2020 and 2021 and the change between 2020 and 2021. The atmospheric stability was dominated by class A, with a proportion of 65.62 and 71.08, respectively. Compared with 2020, the atmospheric stability class A increased by 5.46% in 2021. In contrast, the class B, C, D, E, and F decreased in 2021, ranging from 0.26% to 3.58%. The change in atmospheric stability indicated that the pollutants dispersed more easily across wide geographic areas in 2021.

Table 3. Proportion and variation of atmospheric stability in 2020 and 2021 [%]

Year	A	B	C	D	E	F
2020	65.62	14.25	1.02	13.31	1.24	4.45
2021	71.08	13.99	0.75	9.73	0.98	3.46
Change	5.46	–0.26	–0.27	–3.58	–0.26	–0.99

The 3-D joint frequencies with the combination of wind direction, wind speed and atmospheric stability were used as the input parameters to calculate the individual effective dose. Table 4 shows the joint frequency based on the wind speed and atmospheric stability. From tab. 4, the joint frequency between 2020 and 2021 changed a little. Under the condition of an unstable atmosphere and high wind speed, the pollutant was easier to diffuse and thus the adverse pollution level would decrease. As shown in tab. 4, the joint frequency with atmospheric stability class A and wind speed between 1 m/s and 2 m/s increased by about 12% in 2021. It suggested that the meteorological environment was more suitable for pollutant dispersion.

Table 4. The joint frequency based on wind speed and atmospheric stability

	Wind speed [ms^{-1}]	A	B	C	D	E	F
2021	< 1	8.130	0.732	0.000	1.132	0.000	0.000
	1~2	62.950	4.025	0.000	6.770	0.000	0.000
	2~3	0.000	7.936	0.229	0.743	0.046	3.465
	3~5	0.000	1.292	0.492	0.915	0.938	0.000
	5~6	0.000	0.000	0.023	0.149	0.000	0.000
	> 6	0.000	0.000	0.011	0.023	0.000	0.000
Change	< 1	-6.544	0.003	0.000	–1.543	0.000	0.000
	1~2	12.005	0.359	0.000	–0.687	0.000	0.000
	2~3	0.000	–0.386	-0.124	–0.987	0.023	–0.986
	3~5	0.000	–0.245	-0.146	–0.315	–0.383	0.000
	5~6	0.000	0.000	0.000	–0.033	0.000	0.000
	> 6	0.000	0.000	0.000	–0.011	0.000	0.000

Dose calculation

In this study, we took the radionuclide U-234 as an example to analyze its efficiency. Figures 1 and 2 show the air concentration and its change in 16 directions within the overall assessment region. From fig. 1, as the distance from the center increased, the air concentration in all directions decreased. For all directions, the air concentration reached the peak within 0~1 km and decreased dramatically with the distance of 1~2 km. As the air concentration was greatly related to the individual dose, it was inferred that the individual dose could be the highest within 0~1 km. In addition, the difference among different distances was the highest within 0~1 km. There was little difference among different distances beyond 10 km. The maximum air concentration was observed in the NNW direction around 0~1 km, with a value of 1.93×10^{-7} Bq/m^3.

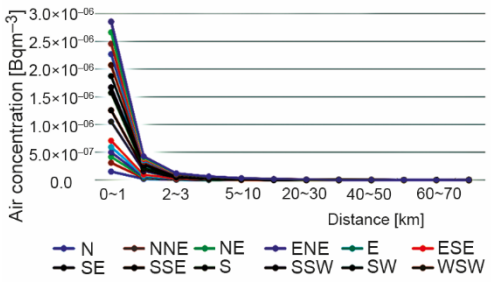

Figure 1. Air concentration for U-234 in 16 directions in 2021

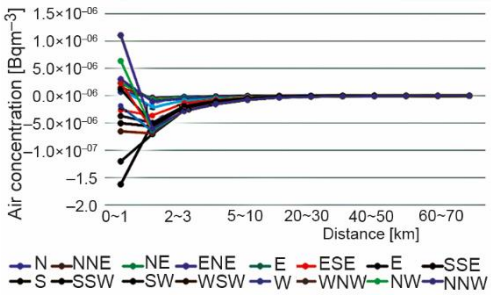

Figure 2. Air concentration change for U-234 in 16 directions between 2020 and 2021

Affected by the meteorological parameters change such as wind direction, wind speed and atmospheric stability, air concentration for U-234 changed between 2020 and 2021. It was evident for the distance within 0~1 km. Air concentration for U-234 decreased in the direction of E, ESE, SE, SSE and SSW in 2021 compared with 2020. In contrast, it increased in other directions. In addition, the change reached the peak within the 0~1 km distance. In contrast, it decreased dramatically with the increasing distance. There was little difference among different distances beyond 10 km.

Figure 3 shows the individual dose at different distances within the assessment area in 2021. From fig. 3, it was evident that the individual dose was the highest at the distance of 0~1 km from the released source point. The individual dose was the highest for the adult with the value of 4.46×10^{-7} Sv per year, whereas it was the lowest for the infant with the value of 1.67×10^{-7} Sv per year. As the distance from the center increased, the individual dose gradually decreased. It was mainly attributed to the pollutant dispersion feature. The individual dose change was particularly evident from the distance of 0~1 km to 1~2 km. For instance, the individual dose for adult group decreased from 4.46×10^{-7} Sv per year at the distance of 0~1 km to 7.19×10^{-8} Sv per year at the distance of 1~2 km.

Figure 4 shows the individual dose change between 2020 and 2021. For all age groups, the individual dose in 2021 was significantly higher than that in 2020 at the distance of 0~1 km. In contrast, the individual dose in 2021 was lower than that in 2020 beyond 1 km. This phenomenon was consistent with the change in air concentration in fig. 2. As shown in fig. 4, the difference of the individual dose between 2020 and 2021 was positive and reached

its peak in 0~1 km. It was negative beyond the distance of 0~1 km. In addition, the difference gradually decreased with the increasing distance. There was not significant difference beyond the 10 km. Among four age groups, the difference was the most evident for the adult group. It indicated that the radiological environmental impact under meteorological variations should not be neglected at a closer distance.

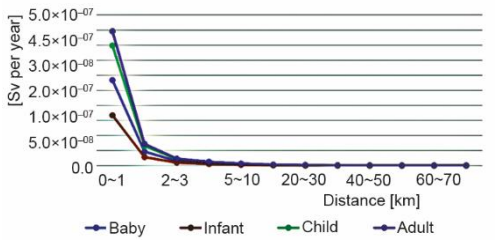

Figure 3. Individual dose at different distances in 2021

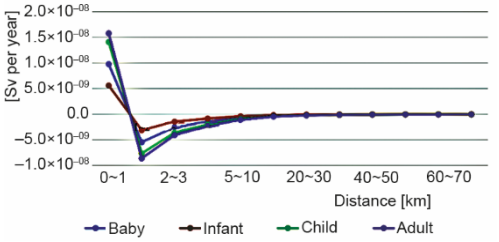

Figure 4. Individual dose change between 2020 and 2021

The individual effective doses for different pathways (inhalation, ground-shine, immersion and ingestion) from the release point were calculated based on the dose evaluation model. As already mentioned, there were no people inhibited within 5 km. Based on the individual dose at different distances in fig. 3, the maximal individual effective dose was observed at around 5~10 km. Table 5 shows the maximal individual effective dose in 2021 and its change between 2020 and 2021. With regard to the air concentration change shown in fig. 2, the air concentration for U-234 in 2021 was lower than that in 2020 at 5~10 km. As shown in tab. 5, the change of maximal individual effective dose was consistent with that of the air concentration.

With the distance between 5 km and 10 km, the maximal individual effective dose for baby, infant, child, and adult were 1.60×10^{-8} Sv per year, 9.54×10^{-8} Sv per year, 2.30×10^{-8} Sv per year, and 2.56×10^{-8} Sv per year, respectively. The key residential group was the adult. In comparison with different pathways, the critical exposure path was internal exposure from the inhalation, which accounted for 92.2% of the total dose.

Table 5. Maximal individual effective dose [Sv per year] calculation results in 2021

	Immersion	Ground-shine	Inhalation	Ingestion [Crop]	Ingestion [Animal]	Total (2021)	Change
Baby	$5.28 \cdot 10^{-17}$	$1.25 \cdot 10^{-11}$	$1.45 \cdot 10^{-8}$	$1.48 \cdot 10^{-9}$	$2.20 \cdot 10^{-11}$	$1.60 \cdot 10^{-8}$	$-1.80 \cdot 10^{-9}$
Infant	$5.28 \cdot 10^{-17}$	$1.25 \cdot 10^{-11}$	$8.35 \cdot 10^{-9}$	$1.16 \cdot 10^{-9}$	$2.01 \cdot 10^{-11}$	$9.54 \cdot 10^{-9}$	$-1.04 \cdot 10^{-9}$
Child	$5.28 \cdot 10^{-17}$	$1.25 \cdot 10^{-11}$	$2.07 \cdot 10^{-8}$	$2.22 \cdot 10^{-9}$	$3.43 \cdot 10^{-11}$	$2.30 \cdot 10^{-8}$	$-2.60 \cdot 10^{-9}$
Adult	$5.28 \cdot 10^{-17}$	$1.25 \cdot 10^{-11}$	$2.36 \cdot 10^{-8}$	$1.95 \cdot 10^{-9}$	$3.26 \cdot 10^{-11}$	$2.56 \cdot 10^{-8}$	$-3.00 \cdot 10^{-9}$

Conclusions

Based on the hourly meteorological data obtained from the automatic monitoring station, the radiological impact indicated by the air concentration, individual dose and maxi-

mal individual effective dose were analysed and compared between 2020 and 2021. The major conclusions were as follows.

- The frequency of calm wind decreased significantly, from 14.31% in 2020 to 6.02% in 2021.
- The atmospheric stability was dominated by class A in 2021, which increased by 5.46% in comparison with that in 2020.
- The maximum air concentration for U-234 was observed in the NNW direction around 0~1 km.

Under the effect of changing meteorological parameters, the individual dose change was particularly evident from the distance of 0~1 km to 1~2 km. The maximal individual effective dose was observed at around 5~10 km, with a higher dose value in 2021. The change of maximal individual effective dose was consistent with that of the air concentration. The key residential group was the adult and the critical exposure path was internal exposure from inhalation, which accounted for 92.2%of the total dose. These results can provide suggestions for decision-making by comparing the dose results under different climate conditions. A mathematical model for the pollution's diffusion is much needed in future, and the fractal diffusion and the fractional diffusion models are two suitable candidates [7-9].

Acknowledgment

This work was supported by the Youth Foundation of China Institute for Radiation Protection.

References

[1] Alrammah, I., *et al.*, Atmospheric Dispersion Modeling and Radiological Environmental Impact Assessment for Normal Operation of a Proposed Pressurized Water Reactor in the Eastern Coast of Saudi Arabia, *Progress in Nuclear Energy*, *145* (2022), Mar., pp. 1-15
[2] Mei, Y., *et al.*, On the Mountain-River-Desert Relation, *Thermal Science*, *25* (2021), 6B, pp. 4817-4822
[3] Mei, Y., *et al.*, The Yellow River-Bed Evolution: A Statistical Proof of the Mountain-River-Desert Conjecture, *Thermal Science*, *27* (2023), 3A, pp. 2075-2079
[4] Lu, B., *et al.*, Influence of Atmospheric Stability on Air Ventilation and Thermal Stress in a Compact Urban Site by Large Eddy Simulation, *Building and Environment*, *216* (2022), 109049
[5] Albornoz, C. P., *et al.*, Review of Atmospheric Stability Estimations for Wind Power Applications, *Renewable and Sustainable Energy Reviews*, *163* (2022), 112505
[6] Fairuz, A., Sahadath, M. H., Assessment of the Potential Total Effective Dose (TED) and Ground Deposition (GD) Following a Hypothetical Accident at the Proposed Rooppur Nuclear Power Plant, *Applied Radiation and Isotopes*, *158* (2020), 109043
[7] He, J.-H., Qian, M. Y., A Fractal Approach to the Diffusion Process of Red Ink in a Saline Water, *Thermal Science*, *26* (2022), 3B, pp. 2447-2451
[8] Qian, M. Y., He, J.-H., Two-Scale Thermal Science for Modern Life: Making the Impossible Possible, *Thermal Science*, *26* (2022), 3B, pp. 2409-2412
[9] Cetinkaya, S., *et al.*, Solutions for the Fractional Mathematical Models of Diffusion Process, *Facta Universitatis Series: Mechanical Engineering*, *37* (2022), 1, pp. 103-120

Paper submitted: March 31, 2023
Paper revised: August 1, 2023
Paper accepted: August 2, 2023